*Rev. Roum. Sci. Techn.– Électrotechn. et Énerg.*
Vol. **71**, *2*, pp. 281–286, Bucarest, 2026

# PUSH-PULL CONVERTER FOR MILD-HYBRID AUTOMOTIVE APPLICATIONS

CRISTIAN AGHION[1], COSMINA-ELENA ONOFREI[1], NICOLAE LUCANU[1], OVIDIU URSARU[1]

**Keywords: Push-pull converter; Automotive; DC-DC; Ripple; Efficiency.**

**The push-pull converter is an optimal solution for low- and medium-power automotive applications, providing galvanic isolation and simple construction. This paper evaluates the efficiency of a converter designed in a push-pull configuration for the automotive domain, powered by a 24 V ± 6 V input and delivering a 48 V output. The proposed converter, used in advanced start-stop systems for mild-hybrid and full-hybrid vehicles, operates with variable switching frequencies between 70 kHz and 300 kHz and various power levels. The output voltage ripple is a critical parameter in the design and performance of DC-DC converters, as it directly influences the required output capacitance connected in parallel with the load. Existing analytical expressions for estimating the ripple, normalized to the average output voltage, have primarily been developed under the assumption of continuous conduction mode (CCM) operation. The proper functioning of the converter and the efficiency variation across different operating regimes were validated theoretically, through simulation, and experimentally. This paper proposes a new formula that uses real circuit parameters for determining the efficiency of the push-pull converter. The derived formula has been validated through both simulation and experimental results, demonstrating strong agreement between the theoretical and experimental outcomes. Although it provides accurate results under the analyzed conditions, the proposed formula can be further improved by including additional factors specific to real operating conditions.**

## 1. INTRODUCTION

In many applications, and especially in switch-mode power supplies, galvanic isolation between the input and output voltage is required. This isolation is achieved by means of a small-sized high-frequency transformer.

Galvanic isolation is necessary both for electrical safety reasons and for electromagnetic compatibility. It is also beneficial when the output voltage is significantly different from the input voltage. By using a proper turns ratio, the duty cycle operating range of the converter can be optimized.

The push-pull converter is a converter variant that can provide, at the output, voltages either lower or higher than the supply voltage, depending on the transformer conversion ratio. Supplied from a 24 V ± 6 V battery, this converter can efficiently provide a constant 48 V output, which is increasingly used in mild-hybrid and full-hybrid vehicles to power loads such as electric power steering, air conditioning compressors, electric pumps, lighting systems, or advanced start-stop systems [1,2].

The push-pull converter, designed to comply with certain automotive standards, is intended for loads up to 250 W. The evaluation of efficiency performed through simulation, experimental determination, and theoretical calculation (eq. (16), below), aims to anticipate from the design stage the variation margin of the efficiency between the calculated and measured values. Compared to the cases analyzed in [3,4], in this case, the analysis is performed over a switching frequency range from 70 kHz to 300 kHz, at different output power values.

The output voltage ripple is an important parameter of DC-DC converters, based on which the value of the capacitor connected in parallel with the load is determined. Known relations exist for determining the ripple normalized to the average output voltage ($\Delta v_0/V_0$) for ideal DC-DC converters operating in continuous conduction mode (CCM) [5–12]. The expression of the normalized peak-to-peak output voltage ripple of the converter is doubled depending on the frequency of the current through the inductance and, therefore, also through the capacitor.

## 2. DETERMINATION OF THE PUSH-PULL CONVERTER EFFICIENCY USING AVERAGE-VALUE EQUIVALENT CIRCUITS

The schematic diagram of the push-pull converter is presented in Fig. 1. To determine the average-value equivalent circuits (DC current) and the corresponding equations, the analysis starts from the ideal operating conditions of the circuit [6].

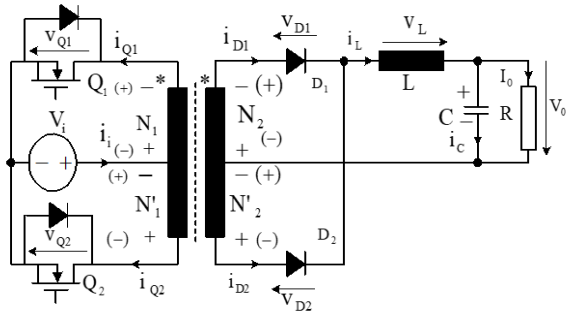


Fig. 1 – Push–pull converter circuit

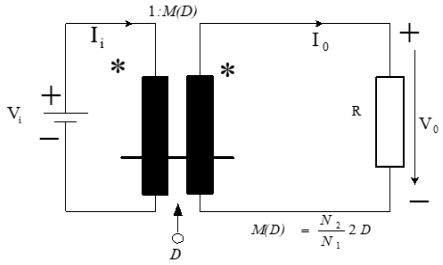


Fig. 2 – Average-value equivalent circuit of the ideal push–pull converter operating in CCM using the ideal DC transformer model.

The expression of the current $i_i$ delivered by the source $V_i$ [6]:

$$i_i = i_{Q1} + i_{Q2}, \tag{1}$$

a relation that also holds for the average currents' values [6]:

$$I_i = I_{Q1AVR} + I_{Q2AVR} = 2I_{QAVR}. \tag{2}$$

The average current through the transistor (equal to the average current through the winding $N_1$) is [6]:

[1]Faculty of Electronics, Telecommunications and Information Technology, "Gh. Asachi" Technical University, Iasi, Romania.
E-mail:aghion@etti.tuiasi.ro,cosmina.onofrei@etti.tuiasi.ro, nlucanu@etti.tuiasi.ro,ovidiu@etti.tuiasi.ro

DOI: 10.59277/RRST-EE.2026.2.19

$$I_{Q1AVR}=I_{N1AVR}=\frac{N_2}{N_1}DI_L=\frac{N_2}{N_1}\frac{DV_0}{R}. \quad (3)$$

Therefore, the average current is [6]:

$$I_i=\frac{N_2}{N_1}2DI_L=\frac{N_2}{N_1}2DI_0\,. \quad (4)$$

The conversion characteristic is [6]:

$$V_0=\frac{N_2}{N_1}2DV_i\,. \quad (5)$$

The last two relations lead us to the average-value (DC) equivalent circuit of the ideal push-pull converter operating in CCM, as shown in Fig. 2. This circuit only provides the average values of the converter's voltages and currents.

The average-value equivalent circuit of the real push–pull converter is derived next, considering the inductor copper losses—modeled by the resistance $R_L$—and the conduction losses in the transistors, each modeled by a resistance $R_{on}$, as well as the losses in the diodes $D_1$ and $D_2$, each represented by a resistance $R_D$ and a voltage source $V_D$

During the first interval $t \in [0, DT]$, the equivalent circuit is the one shown in Fig. 3(a), from which the following equations result for the current supplied by the input source $V_i$ and for the voltage across the inductance $L$.

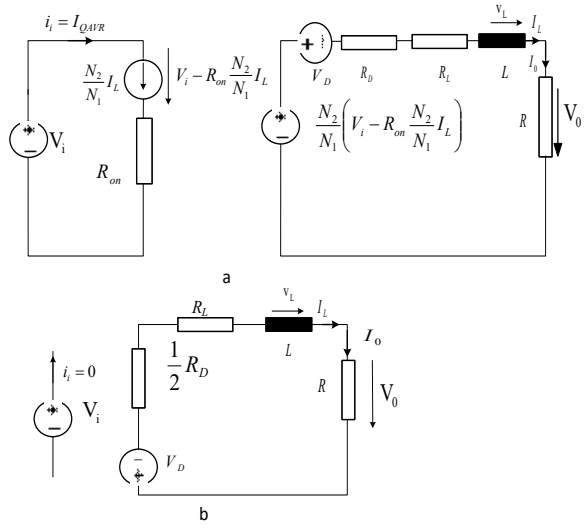


Fig. 3 – Equivalent circuits of the real push–pull converter operating in CCM: (a) $t \in [0, DT]$; (b) $t \in [DT, T/2]$.

The average transistor current is calculated as [6]:

$$I_{Q1AVR}=\frac{N_2}{N_1}I_L;\ t\in[0,DT], \quad (6)$$

$$V_L=\frac{N_2}{N_1}\left(V_i-R_{on}\frac{N_2}{N_1}I_L\right)-(R_D+R_L)I_L-V_D-V_0. \quad (7)$$

During the second interval $t\in[DT,(T/2)]$, if the magnetizing current is neglected, diodes $D_1$ and $D_2$ appear connected in parallel, and the equivalent circuit is that in Fig. 3(b), from which the following equations are derived.

$$i_i=0,\ t\in\left[DT,\frac{T}{2}\right],$$
$$V_L=-\left[V_0+V_D+\left(R_L+\frac{1}{2}R_D\right)I_L\right]. \quad (8)$$

During the other half-cycle, in the third and fourth conduction intervals, the operation is similar, and equivalent circuits identical to those in Fig. 3 are obtained. For this reason, the average-value equivalent circuit of the real converter can be determined using only the equations from the first two intervals. The waveforms of the $i_s$ and $v_L$ shown in Fig. 4.

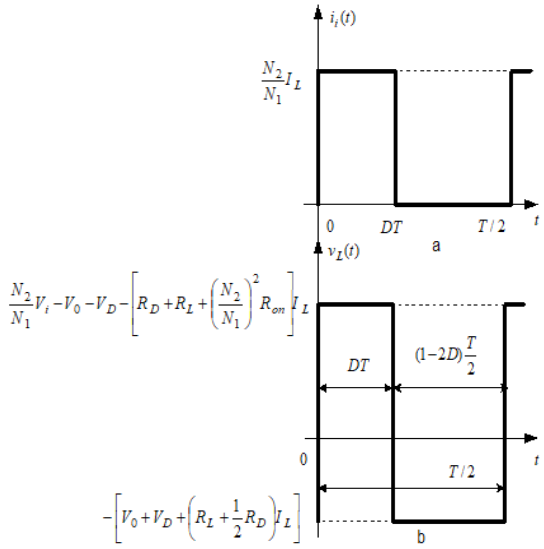


Fig. 4 – Waveforms of the real push–pull converter operating in CCM: (a) source current, (b) voltage across the inductance $L$.

From Fig. 4(a), the following relation is obtained for the average value of the current supplied by the input source $V_i$.

$$I_i=\frac{2}{T}\int_0^{DT}\frac{N_2}{N_1}I_L\mathrm{d}t=\frac{N_2}{N_1}2DI_L=\frac{N_2}{N_1}2DI_0. \quad (9)$$

By applying the waveform $v_L$ in Fig. 4(b) and using the volt-second balance principle, the following relation is obtained:

$$DT\left\{\frac{N_2}{N_1}V_i-V_0-V_D-\left[R_D+R_L+\left(\frac{N_2}{N_1}\right)^2R_{on}\right]I_L\right\}= \\ =\left(\frac{1}{2}-D\right)T\left[V_0+V_D+\left(R_L+\frac{1}{2}R_D\right)I_L\right]. \quad (10)$$

After performing the calculations in eq. (10), the following relation is obtained:

$$\frac{N_2}{N_1}2D\left(V_i-\frac{N_2}{N_1}R_{on}I_L\right)=\frac{N_2}{N_1}2D\left(V_i-\frac{1}{2D}R_{on}I_i\right)= \\ =V_0+V_D+\left(\frac{1}{2}+D\right)R_DI_L+R_LI_L. \quad (11)$$

Equations (8) and (10) lead to the average-value DC equivalent circuit of the real push–pull converter operating in CCM, which uses the ideal DC transformer model shown in Fig. 5. From Eq. (11), considering that $I_L = I_o$, the following relation is obtained:

$$\frac{N_2}{N_1}2DV_i=V_0+V_D+\left(\frac{1}{2}+D\right)R_DI_0+R_LI_0+ \\ +\left(\frac{N_2}{N_1}\right)^2 2DR_{on}I_0. \quad (12)$$

This equation corresponds to the circuit in Fig. 5a. The same circuit can also be obtained by reflecting the primary-side resistance to the secondary side. Figure 5b provides the following relation:

$$V_0=\frac{R\left(\frac{N_2}{N_1}2DV_i-V_D\right)}{R+\left(\frac{1}{2}+D\right)R_D+R_L+2DR_{on}\left(\frac{N_2}{N_1}\right)^2}. \quad (13)$$

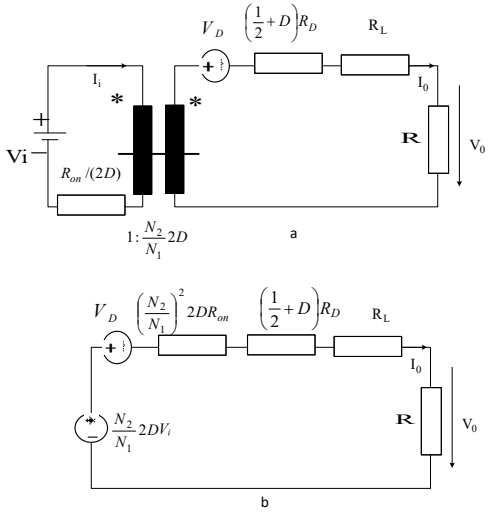


Fig. 5 – (a) Average-value equivalent circuit of the real push–pull converter operating in CCM using the ideal DC transformer model; (b) equivalent circuit of the real push–pull converter in CCM used to derive the conversion ratio M(D) = $V_0/V_i$.

From the last relation, the conversion ratio of the real push–pull converter operating in CCM is obtained:

$$\mathrm{M}(D)=\frac{V_0}{V_i}= \\ =1-\frac{N_1}{N_2}\frac{1}{2D}\frac{V_D}{V_i} \\ =\frac{N_2}{N_1}2D\frac{1}{1+\frac{1}{R}\left[\left(\frac{1}{2}+D\right)R_D+R_L+2DR_{on}\left(\frac{N_2}{N_1}\right)^2\right]}. \tag{14}$$

Compared to the conversion ratio of the ideal push–pull converter, two correction terms appear: the one in the numerator is due to the voltage drop across the diodes during conduction; the one in the denominator is due to the loss resistances of the transistors, the inductance, and the diodes.

The efficiency of the real push–pull converter operating in CCM is calculated using the following relation:

$$\eta=\frac{V_0I_0}{V_iI_i}=\frac{N_1}{N_2}\frac{1}{2D}\frac{V_0}{V_i}= \\ =\frac{1-\frac{N_1}{N_2}\frac{1}{2D}\frac{V_D}{V_i}}{1+\frac{1}{R}\left[\left(\frac{1}{2}+D\right)R_D+R_L+2DR_{on}\left(\frac{N_2}{N_1}\right)^2\right]}. \tag{15}$$

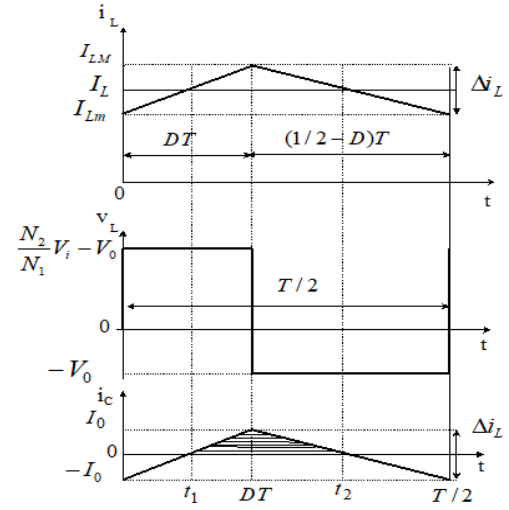


Fig. 6 – Waveforms of the forward converter in CCM mode a) the current through the inductor $i_L$ b) the voltage through the inductor $V_l$; c) current through IC capacitor.

Thus, the same terms that reduce the output voltage also decrease efficiency. Clearly, the efficiency will be higher when the voltage drop across the diodes is lower and when the resistances modeling the losses are minimized.

Figure 6 presents the waveforms of the main quantities involved in the operation of the ideal forward converter in continuous conduction mode (CCM).

Considering the average voltage across the inductor as zero, the regulation characteristic of the converter is:

$$\left(\frac{N_2}{N_1}V_i-V_0\right)DT=V_0\left(\frac{1}{2}-D\right)T \Rightarrow \\ \Rightarrow M(D)=\frac{V_0}{V_i}=2\frac{N_2}{N_1}D. \tag{16}$$

In steady-state operation, the current through the inductor is:

$$I_{Lm}=I_{LM}-\frac{V_0}{L}\left(\frac{T}{2}-DT\right), \\ \Delta i_L=I_{LM}-I_{Lm}=\frac{V_0}{2fL}(1-2D). \tag{17}$$

The average current through the inductor is:

$$I_L=\frac{1}{2}(I_{Lm}+I_{LM})=I_0=\frac{V_0}{R}=\frac{N_2}{N_1}\frac{2DV_i}{R}, \tag{18}$$

From Eq. (18) it follows that:

$$\Delta i_L=\frac{(1-2D)V_0}{2fL}=\frac{N_2}{N_1}\frac{D(1-2D)V_i}{fL}. \tag{19}$$

From eq. (18) and (19) it results that the normalized peak-to-peak ripple of the current through the inductor is:

$$\frac{\Delta i_L}{I_L}=\frac{\Delta i_L}{I_0}=\frac{(1-2D)R}{2fL}. \tag{20}$$

The figure also shows the waveform of the current through the capacitor, whose ripple is $\Delta i_L$:

$$i_C(\mathrm{t})=i_L(t)-I_0. \tag{21}$$

The capacitance is calculated based on Fig. 6. The hatched area represents the electric charge, expressed by the following relation:

$$\Delta q=\int_{t_1}^{t_2}i_C\,\mathrm{d}t=C(\Delta V_0). \tag{22}$$

The capacitance expression is therefore obtained as follows:

$$\frac{\Delta v_0}{V_0}=\frac{1-D}{8(2f)^2LC}\Rightarrow C=\frac{1-D}{32f^2L(\frac{\Delta v_0}{V_0})}. \tag{23}$$

As in the case of the buck converter, the same relationship is used to determine the capacitance C; however, the frequency of the current flowing through the capacitor is doubled.

## 3. ANALYSIS, SIMULATION, AND EXPERIMENTAL RESULTS

The analysis of the converter's operation and the evaluation of its efficiency under varying switching frequency and load resistance conditions were carried out through simulation, experimental verification, and theoretical calculations.

The determination of the normalized output voltage ripple $\Delta v_0/V_0$ is a key design parameter. Its variation with frequency

imposes constraints on the optimization of DC-DC converters [13].

The design and experimental validation of the push–pull converter were carried out under the following conditions: input voltage varied between $V_{in\_min}$ = 18 V and $V_{in\_max}$ = 32 V, output voltage was constant at $V_o$ = 48 V, maximum output current was $I_o$ = 5 A, switching frequency $f_c$ ranged from 70 kHz to 300 kHz, and the normalized ripple $\Delta v_o/V_o$ was maintained below 0.5%.

Table 1 presents the specifications of the main circuit elements used in simulation, experimental verification, and theoretical determination.

*Table 1*

Circuit elements used in simulation, experimental testing, and theoretical analysis.

| Device | Simulation (OrcadPSpice) | Practical implementation |
|---|---|---|
| Transistor | IRFP150 | IRFP150, $R_{ds}$(on)=0.036 Ω |
| Diode | MBR360 | STTH6002C, Rd=0.08 Ω |
| Inductor | Library model (ideal) | ETD29/100u, RL=0.047 Ω |
| Capacitor | Library model (ideal) | 47µF (GRM32ER7YA106KA12) |
| Control | Library model ($V_{pulse}$) | UC3525 |
| Power supply | Library model (ideal) | ZHAOXIN DC Power Supply KXN-6020D |
| Load | Library model (ideal) | Electronic Load EA-EL 3080-60B 0-80V 0-400W |
| Oscilloscope | Library model (ideal) | GWINSTEK GDS-10548, 50MHz, 1 GS/s |
| Current probe | Library model (ideal) | Clamp on probe Rigol RP1003C, 50 MHz, 30 A |

Table 2 presents the efficiency values determined theoretically (using the equation proposed in (15)), experimentally, and through simulation, as a function of the switching frequency *fc*. The output power is $P_{out}$ = 50 W and $P_{out}$ = 100 W, respectively. The output voltage is $V_o$ = 48 V, while the input voltage is $V_i$ = 24 V.

*Table 2*

Theoretical efficiency calculation and experimental determination.

| Switching frequency $f_c$ [kHz] | $P_{out}$ = 56 W Theoretic efficiency | $P_{out}$ = 56 W Experimental efficiency | $P_{out}$ = 100 W Theoretic efficiency | $P_{out}$ = 100 W Experimental efficiency |
|---|---|---|---|---|
| 80 | 0.882 | 0.871 | 0.984 | 0.907 |
| 100 | 0.879 | 0.868 | 0.981 | 0.877 |
| 120 | 0.866 | 0.858 | 0.980 | 0.867 |

Table 3 presents the efficiency values determined theoretically (from eq. (15)), experimentally, and through simulation, as a function of the switching frequency $f_c$. The output voltage is $V_o$ = 48 V, the input voltage is $V_i$ = 30 V, the output current is $I_o$ = 1.5 A, and the output power is $P_{out}$ = 72 W.

*Table 3*

Theoretical efficiency calculation and experimental determination.

| Switching frequency $f_c$ [kHz] | $V_0$ = 48 V, $I_0$ = 1.5 A, $V_i$ = 30 V, $P_{out}$ = 72 W Theoretic efficiency | Experimental efficiency | Efficiency by simulation |
|---|---|---|---|
| 100 | 0.981 | 0.888 | 0.951 |
| 150 | 0.981 | 0.867 | 0.917 |
| 200 | 0.979 | 0.841 | 0.884 |
| 300 | 0.977 | 0.795 | 0.848 |

Table 4 presents the efficiency values determined theoretically (from eq. (15)), experimentally, and through simulation, as a function of the switching frequency *fc*. The output voltage is $V_o$ = 48 V, while the input voltage is $V_i$ = 30 V, the output current $I_o$ = 2.1 A and output power is $P_{out}$ = 100 W.

*Table 4*

Theoretical efficiency calculation and experimental determination.

| Switching frequency $f_c$ [kHz] | $V_0$ = 48 V, $I_0$ = 2.1 A, $V_i$ = 30 V, $P_{out}$ = 100 W Theoretic efficiency | Experimental efficiency | Efficiency by simulation |
|---|---|---|---|
| 100 | 0.973 | 0.862 | 0.925 |
| 150 | 0.971 | 0.839 | 0.901 |
| 200 | 0.971 | 0.813 | 0.869 |
| 300 | 0.970 | 0.771 | 0.840 |

Table 5 presents the efficiency values determined theoretically (from eq. (15)), experimentally, and through simulation, as a function of the switching frequency $f_c$. The output voltage is $V_o$ = 48 V, while the input voltage is $V_i$ = 30 V, the output current $I_o$ = 2.5 A, and the output power is $P_{out}$ = 120 W.

*Table 5*

Theoretical efficiency calculation and experimental determination.

| Switching frequency $f_c$ [kHz] | $V_0$ = 48 V, $I_0$ = 2.5 A, $V_i$ = 30 V, $P_{out}$ = 120 W Theoretic efficiency | Experimental efficiency | Efficiency by simulation |
|---|---|---|---|
| 100 | 0.971 | 0.844 | 0.912 |
| 150 | 0.971 | 0.814 | 0.871 |
| 200 | 0.970 | 0.795 | 0.845 |
| 300 | 0.969 | 0.769 | 0.812 |

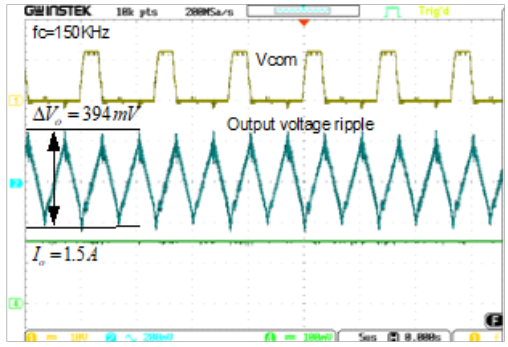


a

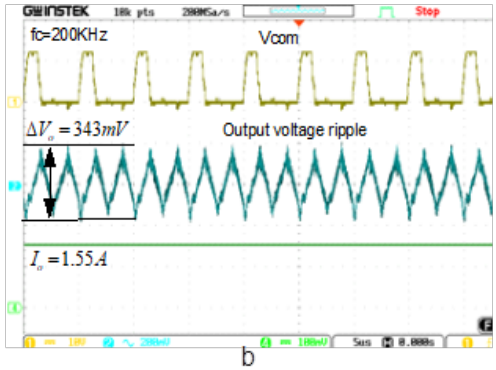


b

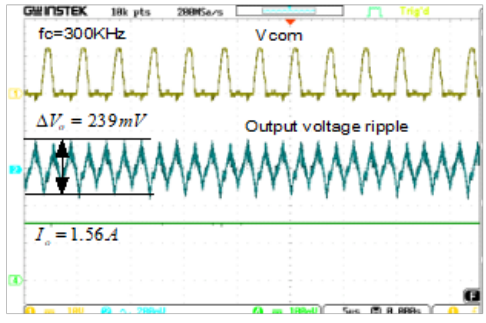


c

Fig. 7 – Waveforms of the control signal $V_{com}$, output voltage ripple $\Delta V_o$, and load current $I_o$, for: a) $f_c$ = 150 kHz; b) $f_c$ = 200 kHz; c) $f_c$ = 300 kHz.

Figure 7 shows the oscilloscope waveforms of the control signal $V_{com}$, the output voltage ripple $\Delta V_0$, and the load current $I_o$. The output power is $P_{out}$ = 72 W, while the switching frequencies $f_c$ are: 150 kHz, 200 kHz, and 300 kHz, respectively.

Table 6 presents the normalized output voltage ripple ($\Delta v_0/V_0$) as a function of switching frequency, calculated from the experimental measurements shown in Fig. 7.

*Table 6*

Experimental determination of $\Delta v_0/V_0$.

| Normalized output voltage ripple | $V_0$ = 48 V, $I_0$ = 1.5 A, $V_i$ = 30 V, $P_{out}$ = 72 W | | |
|---|---|---|---|
| | $f_c$ =150 kHz | $f_c$ =200 kHz | $f_c$ =300 kHz |
| ($\Delta v_0/V_0$) | 0.0084 | 0.0073 | 0.0051 |

Figure 8 shows the oscilloscope waveforms of the output voltage ripple $\Delta V_0$, the control signal for one of the transistors in the converter $V_{com}$, and the load current $I_0$, for load powers $P_{out}$ = 100 W and $P_{out}$ = 120 W, at a switching frequency of $f_c$ = 300 kHz.

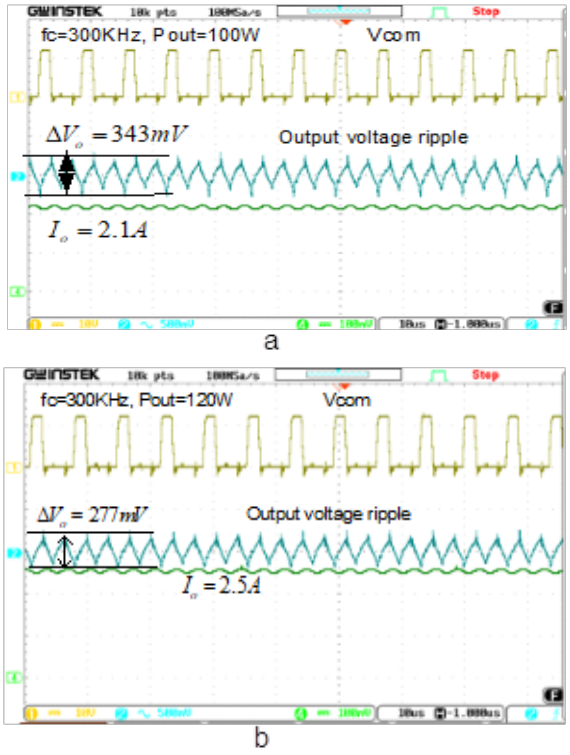


Fig. 8 –Waveforms of the control signal Vcom, output voltage ripple $\Delta V_0$, and load current $I_o$, for: a) *Pout* = 100 W, b) *Pout* = 120 W.

Using the oscilloscope waveforms from Fig. 8, Table 7 presents the values of the output voltage ripple normalized to the average output voltage $\Delta v_0/V_o$, calculated for $P_{out}$ = 100 W and $P_{out}$ = 120 W, with $V_0$ = 48 V and a switching frequency of $f_c$ = 300 kHz.

*Table 7*

Experimental Determination of $\Delta v_0/V_i$.

| Normalized output voltage ripple | $V_0$ = 48 V, $V_i$ =30 V, $f_c$ = 300 kHz | |
|---|---|---|
| | $P_{out}$ = 100 W | $P_{out}$ = 120 W |
| ($\Delta v_0/V_0$) | 0.0073 | 0.0059 |

Figure 9 presents the graphs of the experimentally determined efficiency as a function of the load current $I_o$ for 1.5 A, 2.1 A, and 2.5 A, and for switching frequencies of 100 kHz, 150 kHz, 200 kHz, and 300 kHz.

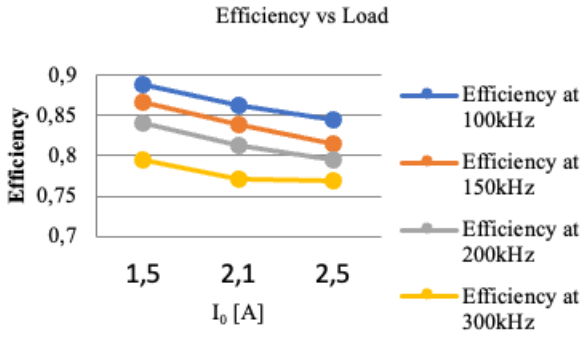


Fig. 9 – Efficiency variation as a function of switching frequency, depending on load current.

Figure 10 presents the experimental push-pull converter circuit, the power supply, oscilloscope, active load, and current probe.

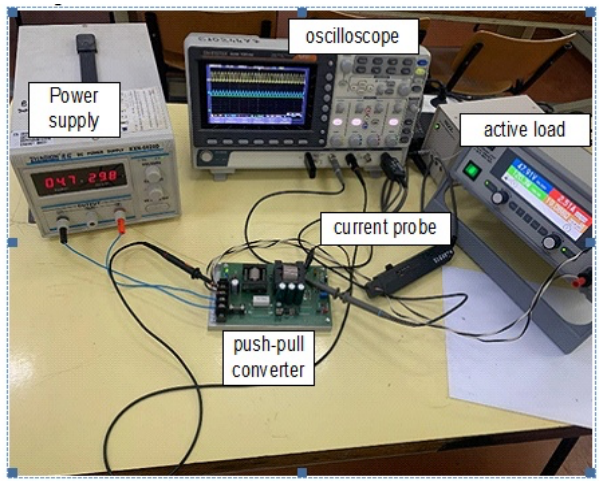


Fig. 10 – Experimental push-pull converter circuit

## 4. CONCLUSIONS

In the context of mild-hybrid automotive applications, the push-pull converter is an efficient solution for DC-DC conversion, especially when energy transfer between voltage rails is required, *e.g.*, 12/24 V – 48 V or 400 V – 48 V. The efficiency values determined experimentally range between 91% - 80%, depending on power and switching frequency.

In the range of 70 kHz - 120 kHz, the analyzed converter offers an efficiency 3-4 percent higher than that of similar converters [2].

An important aspect to highlight is the fact that the difference between the theoretically calculated and experimentally determined efficiency is approximately 8.2%, and it remains at this value with minor variations, regardless of whether the output power changes from 56 W to 120 W or the switching frequency varies from 70 kHz to 300 kHz. Maintaining this value constant among the efficiency metrics calculated and determined experimentally under different converter operation scenarios confirms the validity of the proposed eq. (15).

The normalized output voltage ripple is set to a standard value of 0.5%, and enforcing a specific ripple value determines the selection of the output capacitance.

The obtained results recommend the use of the push-pull converter in the automotive domain as a solution that can optimize cost, efficiency, and integration flexibility.

The application of the derived formula provides an efficient and reproducible method for determining the results, eliminating the need for complex and costly experimental procedures.

The obtained results open new research directions focused on optimizing and generalizing the calculation formula for power converters operating under various conditions.

## ACKNOWLEDGMENT

The authors would like to acknowledge that this work was carried out within the Faculty of Electronics, Telecommunications and Information Technology at the "Gheorghe Asachi" Technical University of Iași.

*Table 8*

List of symbols

| | |
|---|---|
| $V_i$ | Supply voltage |
| $I_i$ | Input current |
| $I_{QAVR}$ | The average current through the transistor |
| $N_1$ | Number of turns in the primary winding |
| $N_2$ | Number of turns in the secondary winding |
| $V_0$ | Output voltage |
| $I_0$ | Load current |
| $R_L$ | Inductor loss resistance |
| $R_D$ | Diode loss resistance |
| $R_{on}$ | Transistor on-state resistance |
| $D$ | Duty cycle |
| $M(D)$ | Conversion ratio |
| $\eta$ | Efficiency |
| $f_c$ | Switching frequency |
| $P_{out}$ | Output power |
| $\Delta v_0/V_0$ | Normalized output ripple |
| $V_{com}$ | Control signal for one transistor |

## CREDIT AUTHORSHIP CONTRIBUTION STATEMENT

All authors contributed to the conception, analysis, simulations, experimental validation, and preparation of this manuscript.

*Received on 28 July 2025*

## REFERENCES

1. K. Sayed, A. Almutairi, N. Albagami, O. Alrumayh, A.G. Abo-Khalil, H. Saleeb, *A review of DC-AC converters for electric vehicle applications*, Energies, **15**, pp. 1–10 (2022).
2. C.C. Raicu, G.C. Seritian, B.A. Enache, *48 V network adoption for automotive lighting systems*, Rev. Roum. Sci. Techn. – Électrotechn. et Énerg., **66**, *4*, pp. 231–236 (2021).
3. Z. Ivanović, M. Knezic, *Modeling push-pull converter for efficiency improvement*, Electronics, **11**, pp. 1–10 (2022).
4. M. Mirsamadi, M. Taherbaneh, A.H. Rezaie, *Efficiency improvement of a DC-DC converter used in series-connected boost converters*, IEEE Electrical Power & Energy Conference, pp. 1–6 (2010).
5. M.H. Rashid, *Power Electronics Handbook*, Elsevier, Amsterdam, The Netherlands, pp. 213–223 (2018).
6. M. Lucanu, N. Lucanu, O. Ursaru, *Convertoare de curent continuu pentru surse în comutație*, Ed. PIM, Romania, pp. 104–122 (2021).
7. S.L. Liu, J. Liu, H. Mao, Y.Q. Zhang, *Analysis of operating modes and output voltage ripple of DC-DC converters and their design considerations*, IEEE Trans. Power Electron., **23**, pp. 1813–1821 (2008).
8. L. Shulin, L.Van, L. Li, *Analysis of output voltage ripple of DC-DC converter and its design*, Proc. PEITS, **2**, pp. 112–115 (2009).
9. S.L. Liu, Y. Liu, L. Liu, *Operational modes and output-voltage-ripple analysis and design considerations of buck-boost DC-DC converters*, IEEE Trans. Ind. Electron., **59**, pp. 381–391 (2012).
10. G. Moschopoulos, *DC-DC converter topologies: Basic to advanced*, Wiley-IEEE Press, Hoboken, NJ, USA, pp. 63–82 (2023).
11. T.H. Van, T. Le Van, T.M.N. Thi, M.Q. Duong, G.N. Sava, *Improving the output of DC-DC converter by phase shift full bridge applied to renewable energy*, Rev. Roum. Sci. Techn. – Électrotechn. et Énerg., **66**, *3*, pp. 175–180 (2021).
12. T.I. Voicila, G.C. Seritian, B.A. Enache, *Analysis of bidirectional DC-DC power converters for screening systems of retired batteries*, Rev. Roum. Sci. Techn. – Électrotechn. et Énerg., **69**, *3*, pp. 311–316 (2024).
13. C.L. Wei, M.H. Shih, *Design of a switched-capacitor DC-DC converter with a wide input voltage range*, IEEE Trans. Circuits Syst., **60**, pp. 1648–1656 (2013).